Free-surface Profiles and Turbulence Characteristics in Skimming Flows along Stepped Chutes

André Luiz Andrade Simões[1], Harry Edmar Schulz[2, 3], Rodrigo de Melo Porto[3], John Stephen Gulliver[4]

[1]Dept. Civil Engg., University Salvador, Av. Juracy Magalhães Junior, 105, CEP 41940-060, Salvador, BA, Brazil
[2]Nucleus of Thermal Sciences & Engg., University of São Paulo, Av. do Trabalhador São-carlense, 400, CEP 13566-590, São Carlos, S.P., Brazil
[3]Dept. Hydraulics & Sanitary Engg., University of São Paulo, Av. do Trabalhador São-carlense, 400, CEP 13566-590, São Carlos, S.P., Brazil
[4]Saint Anthony Falls Lab., Dept. Civil Engg., University of Minnesota, 2 Third Avenue SE, MN 55414, USA
[1]andre.simoes@pro.unifacs.br; [2]harry.schulz@pq.cnpq.br; [3]rodrigo@sc.usp.br; [4]gulli003@umn.edu

Abstract- **The behavior of the free surface in skimming flows along stepped chutes is investigated for the step ratio 1V:1H. Data were collected using high frequency ultrasound probes. The measurements included mean surface profiles, statistical parameters related to the surface position, aeration inception point, water depth at the inception point and transition length. The measurements were related to turbulence parameters at the free surface. The measurement methodology was adequate for both the black-water and the white-water regions. Characteristic relations are developed for different variables defined for skimming flows. The results demonstrate regions of increasing and decreasing turbulence in the transition between the black-water and the white-water flows, and a region of decay of turbulence, related to the distance needed to attain the quasi-uniform flow of the white-water.**

Keywords- Air-Water Free Surfaces; Stepped Chutes; Turbulence; Skimming Flows; Multiphase Flows

I. INTRODUCTION

The behavior of the variables that characterize multiphase flows along stepped chutes, and the economic attractiveness of using stepped spillways, have motivated research on topics related to these flows. Of interest are the location of the air entrainment inception point on the spillway, the water depth, near-surface turbulence intensities after aeration inception and the transition length between black-water and fully aerated flows. Different methods were used to obtain these parameters, by different authors (see, for example, [1] through [9]). However, the measurement and the prediction of the free surface profile downstream of the aeration inception point are still seen as a challenge [10] (p.89), [11] (p.63), [12] (p.82). This study presents high quality experimental results of the behavior of the free-surface in flows along a stepped chute, with 1V:1H for the steps, obtained using ultrasonic displacement meters. The specific objectives of the study are: (a) to provide the position of the inception point for the aeration and the water depth in this position, (b) to measure the shape of the mean free-surface profile, (c) to identify characteristic mean depths, (d) to evaluate turbulent intensities near the free-surface, (e) to evaluate the Strouhal number along the flow, and (f) to correlate the region of decay of the turbulence with the length needed to attain the quasi-uniform flow. It is shown that all this information can be obtained using the ultrasonic displacement meters.

II. EXPERIMENTAL SETUP AND METHODOLOGY

The experiments, conducted in the Laboratory of Environmental Hydraulics of the School of Engineering at São Carlos (University of Sao Paulo), were performed in a stepped chute with width of 0.20 m and a length of 5.0 m, from which 3.5 m were used for the surface measurements. The angle between the pseudo bottom and the horizontal was 45° with a step height and length of 0.05 m. The channel had a pressurized intake, controlled by a sluice gate and the water supply used a motor/pump unit that allowed a maximum flow rate of 0.0833 m^3/s. The flow rate measurements were performed using a rectangular weir located in the outlet channel and an electromagnetic flow meter positioned in the inlet, used for confirmation of the weir discharge measurements.

The position of the free surface was measured using an ultrasonic displacement meter with a resolution of 1 mm and ultrasonic waves of 50 kHz frequency. Previous applications of ultrasound in stepped spillways may be found, for example, in [5] to measure the position of the free surface in a physical model of the Folsom Dam auxiliary spillway. Reference [13] also used acoustic sensors in studies related to hydraulic jumps, while [9] and [14] described the use of ultrasound for the measurement of the transition length between the "full water" and "full mixed" cross-sections in aerated flows.

The acoustic sensor was fixed to a movable longitudinal support, located midway between the right and left sides of the chute, as shown in the left-upper portion of the sketch of Fig. 1a. A view of the chute is shown in Fig. 1b. Along the first 60 cm of the flow, the measurements were made in sections spaced 5 cm apart. After this first 60 cm length, a spacing of 10 cm was adopted. The first longitudinal position, indicated here as x=0, was located downstream of the gate, and was defined as the position where the acoustic sensor did not detect any inlet obstacles. This distance from the inlet was approximately 16.0 cm (+/- 0.2 cm), with 6000 measurements performed using the sample rate of 50 Hz at each position along x. The experimental

flow rates and other conditions related to each of the experiments are shown in Table 1.The terminology of the S_2 and S_3 profiles, used in this Table, was defined by [15].

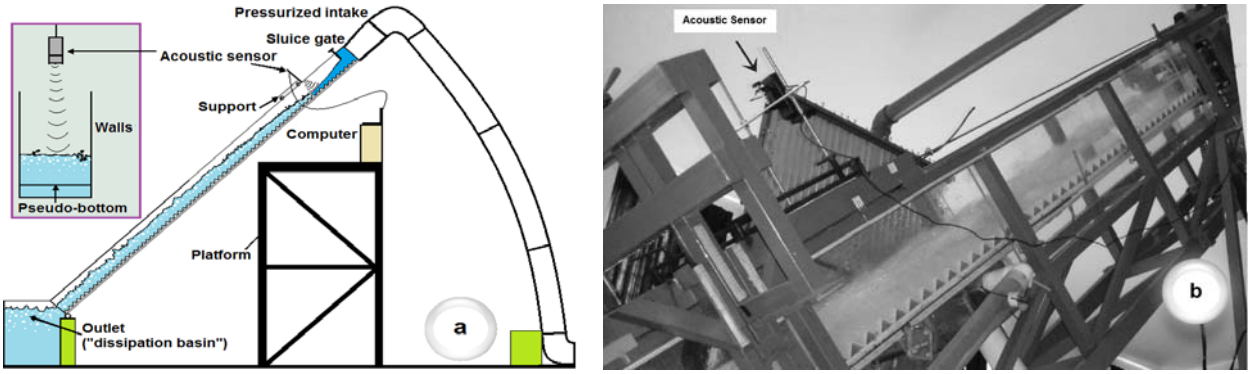

Fig. 1 a) Schematic arrangement of the experiments b) A view of the chute

TABLE I EXPERIMENTAL DATA RELATED TO FLOW CONDITIONS

Number	Experiment name	Q [m^3/s]	Single-phase profile	q [m^2/s]	h_c [m]	s/h_c [-]	h(0) [m]
1	Exp. 2	0.0505	S_2	0.252	0.187	0.268	0.103
2	Exp. 3	0.0458	S_2	0.229	0.175	0.286	0.101
3	Exp. 4	0.0725	S_2	0.362	0.238	0.211	0.106
4	Exp. 5	0.0477	S_2	0.239	0.180	0.278	0.087
5	Exp. 6	0.0833	**S_3**	0.416	0.261	0.192	0.092
6	Exp. 7	0.0504	S_2	0.252	0.187	0.268	0.089
7	Exp. 8	0.0073	S_2	0.0366	0.051	0.971	0.027
8	Exp. 9	0.0074	S_2	0.0368	0.052	0.967	0.024
9	Exp. 10	0.0319	S_2	0.159	0.137	0.364	0.058
10	Exp. 11	0.0501	**S_3**	0.250	0.186	0.269	0.06
11	Exp. 14	0.0608	S_2	0.304	0.211	0.237	0.089
12	Exp. 15	0.0561	S_2	0.280	0.200	0.250	0.087
13	Exp. 16	0.0265	S_2	0.133	0.122	0.411	0.046
14	Exp. 17	0.0487	S_2	0.244	0.182	0.274	0.072
15	Exp. 18	0.0431	S_2	0.216	0.168	0.298	0.074
16	Exp. 19	0.0274	S_2	0.137	0.124	0.402	0.041
17	Exp. 20	0.0360	S_2	0.180	0.149	0.336	0.068
18	Exp. 21	0.0397	S_2	0.198	0.159	0.315	0.071

Q=flow rate; q=Q/B; B=width of the channel; h_c=critical depth; s=step height; h(0)=mean depth at x=0

The free surface flow in stepped chutes is composed by irregular and contorted waves (as in smooth channels, see [16]), ejection of drops, and multiple cavities originated by low pressures on the corners of the steps. These phenomena can be observed with the aid of a strobe or a high speed camera, as shown by [8] and [16]. Fig. 2 contains some photographs and a schematic drawing illustrating the irregular structure of the free surface. Depending on the objectives of the study, a problem may arise when using ultrasound probes for free-surface measurements, related to the detection of ejected liquid parcels.

The ultrasonic sensor correctly measures the distances greater than 0.15 m. The detection of drops out of this limit led to the rejection of samples, which is good for the measurement of the position of the surface, but which must be avoided when measuring the statistical properties of the drops. In order to verify the influence of the position of the drops in the mean profiles, a data rejection criterion was used to construct box plots, i.e., an outlier is a measurement that exceeds qr_1-φIQR and qr_3+φIQR, in which, qr_1 and qr_3 are the first and third quartiles, IQR is the interquartile range and φ is a number, chosen here as 1.5 based on the standard value in statistical analyses [17].

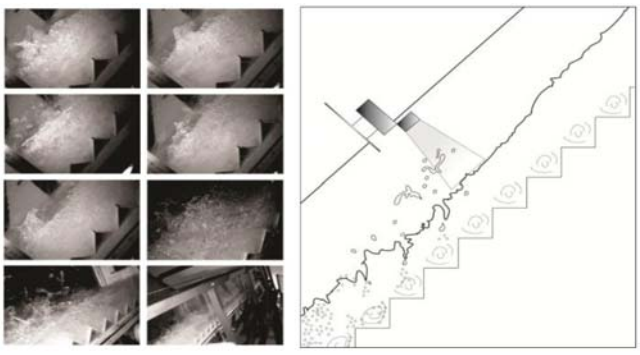

Fig. 2 Free-surface structure

The photos were taken using a 1/40 s shutter speed, with flash. The video was adjusted to 30 fps, not synchronized with the strobe. The best images were chosen from the whole set

In Table 1 the experiments with names Exp. 1, Exp. 12 and Exp. 13 were not considered because Exp. 1 was only a test of the experimental conditions, and during Exp. 12 and Exp. 13 operational problems (affecting for example the water pump used to generate the flow) impeded the maintenance of the experimental conditions.

III. RESULTS AND DISCUSSION

A. Averaged Free Surface Profiles

The shapes of the mean free-surface profiles obtained follow the general characteristics presented in Fig. 3. Note the occurrence of an S_2 profile of accelerating flow, before the inception point is reached, indicated here by the arrow that also defines the position of the depth h_1. The average profile of the two-phase flow has a sinusoidal character, allowing to define three characteristic depths, expressed here as h_1, h_2 and h_3. The undulation corresponding to these three depths was named here "steady biphasic wave". Between h_1 and h_2, bulking of the flow due to air entrainment increases depth to overwhelm the S_2 profile. This is defined as the transition length to a fully aerated flow. For the present experimental conditions, the observations suggest that part of the longitudinal kinetic energy of the S_2 flow was converted into an "excess" of potential energy (the water can be seen, in a simplified manner, as being "launched" vertically during the mixing with air), so that, after h_2, this excess is lost, generating the decreasing region (simply, the water "falls" to the equilibrium position). This result corresponds to visual observation through the sidewalls and calculations using the depth where the temporal mean void fraction is 90%, which also indicates the wavy pattern (see also [6]). The remaining average profiles corresponding to the experiments of Table 1 can be seen in [9], while a rigorous definition of the transition length can be found in [18].

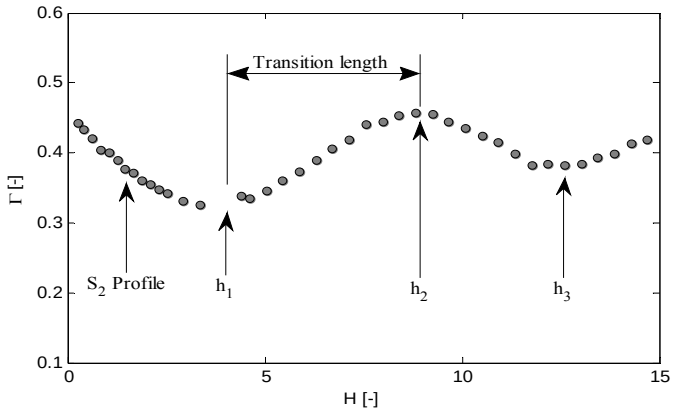

Fig. 3 Time-averaged free-surface profile (Exp. 18)

$\Gamma = \overline{h}/h_c$, $\overline{h}$ =time-averaged depth, H=z/h_c, z=vertical axis with origin at x=0 (the use of z is current in studies of spillways)

The signals of the ultrasonic sensor show distributions of "h" values that depend on the position of the measurement section along the channel. Figs. 4a and 4b show two different signals, both corresponding to Exp. 18, but obtained in the single phase region and in the two-phase flow region, respectively. The distribution of values for the single-phase flow shows a less scattered cloud of points than the two-phase flow. Note that Figs. 4 a, b show asymmetric point distributions. The asymmetry occurs naturally, because the drops are formed only above the surface.

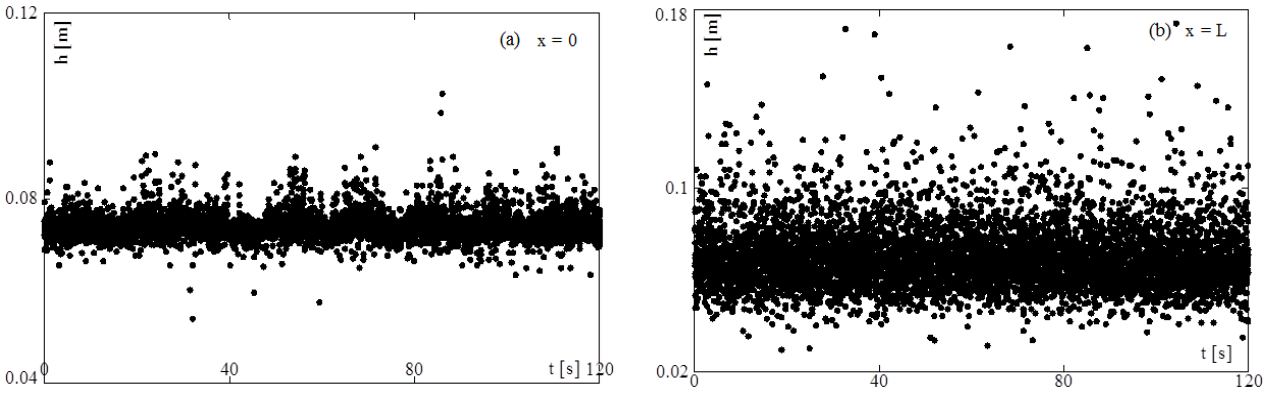

Fig. 4 Values of the measured "depth" *versus* time for two positions along the channel: (a) Values obtained in the region with single-phase flow, (b) Values obtained at the far end of the channel, where the flow is biphasic

The scattering of the measured values is considerably diminished by applying the rejection criterion described herein, as seen in Figs. 5 a and b. Despite this procedure, the average profiles have changed only subtly. For all experiments presented in Table 1, the maximum relative errors for the averaged values resulted less than 5.6%, as seen in Fig. 6 (note that only two experiments showed a maximum change between 3.8 and 5.6%). Additionally, the maximum percentage of rejected samples was 8.3% for Exp. 5, Table I.

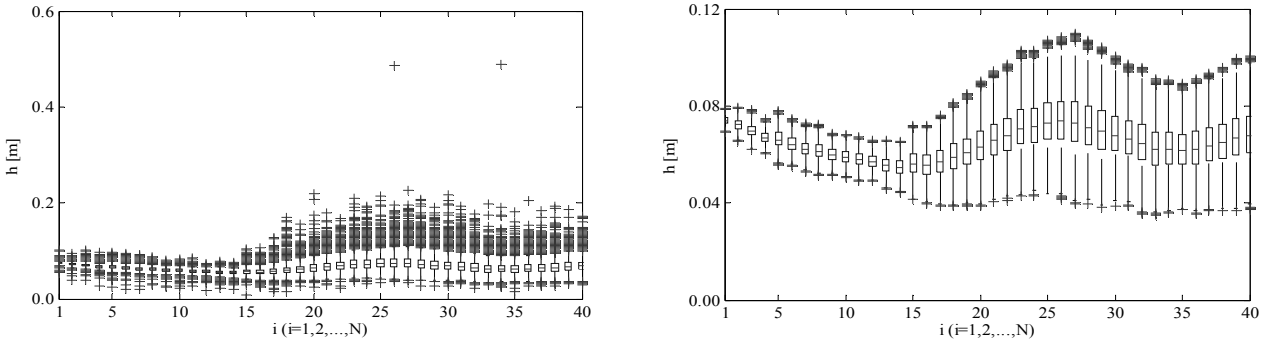

Fig. 5 Exp. 18 Boxplots: (a) with outliers; (b) without outliers (N=40)

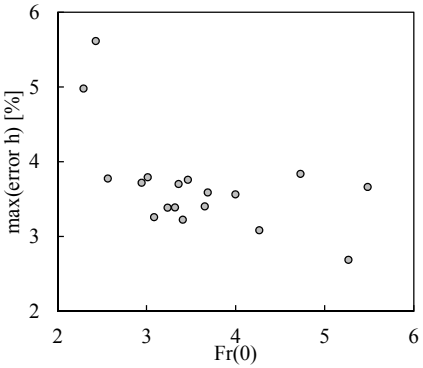

Fig. 6 Maximum relative errors for the time-averaged profiles as plotted against the Froude number $Fr(0)=q/[gh(0)^3]^{1/2}$(parameters defined in Table 1)

B. Characteristic Depths, Transition Lengths and Inception Points

In this section, empirical relationships between relevant parameters for the transition region are presented. The results involve the characteristic depths shown in Fig. 3, obtained for black water S_2 free-surface profiles. Equation 1 was obtained from dimensional arguments, and considering that the two nondimensional parameters h_1/k and F_r^* may be related through a power law, as defined by several authors ([1], [4], [11], [29]).

Adjusting the constants shown in Eq. 1, the obtained correlation coefficient between measured and calculated values was R=0.97. Fig. 7 contains the experimental points obtained in this study, and results of other researchers cited in the caption. Excellent agreement is observed between the results of the different sources and Eq. 1.

$$\frac{h_1}{k} = 0.363F_r^{*0.609}, \tag{1}$$

in which $F_r^*=q/(gk^3\sin\alpha)^{1/2}$, $k=s\cos\alpha$, s is the step height, and the use of Eq. 1 is valid for $2.09\leq F_r^*\leq 20.70$.

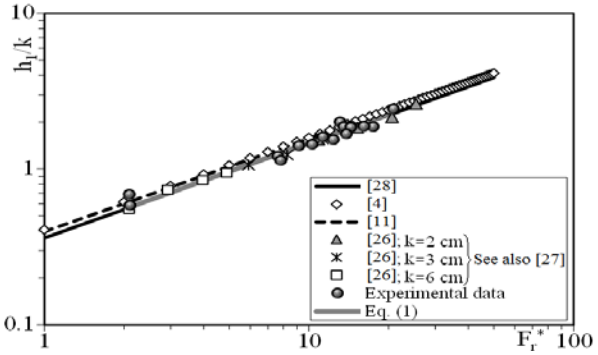

Fig. 7 Superficial inception point depth: comparisons with data from different authors. Note that [11], [26], [27] and [28] used a step ratio of 1V:0.75H ([27] describes numerical CFD techniques also used by [26])

The dimensionless height h_2/k is well connected to h_1/k, also following a power law, shown in Eq. 2, which leads to the correlation coefficient R = 0.99. Finally, the third characteristic length is also related to the first two. Equation 3 expresses the linear relationship that exists between the dimensionless heights h_3/k and h_2/k, also leading to a correlation coefficient R = 0.99.

$$\frac{h_2}{k} = 1.408\left(\frac{h_1}{k}\right)^{0.879}, \tag{2}$$

$$\frac{h_3}{k} = 0.908\frac{h_2}{k} - 0.0748. \tag{3}$$

As can be seen, h_1/k, h_2/k, and h_3/k are related, and can be obtained from the value of F_r^*. Equations 1, 2, and 3 are valid for 1V:1H steps. Equations 2 and 3 were not tested, however, for the 1V:0.75H steps.

Reference [1] studied the flow in a stepped chute with pressurized intake, having defined the beginning of the bed aeration as the cross section where the void fraction near the bottom is equal to 1% (the pseudo bottom is considered, that is, the surface defined by the outer vertices of the steps). References [1] and [2] presented empirical equations to calculate the beginning of the bed aeration for an uncontrolled stepped spillway, for which the condition of pressurized inlet was adjusted (or extrapolated) to represent an uncontrolled spillway, using the energy equation (see [1], p.126). In the present study a similar adjustment (or extrapolation) was used. The resistance factor was calculated using the analytical solution presented by [19], taking the Coriolis coefficient equal to the unity. The semi-empirical equation was then obtained:

$$\frac{Z_S}{s} = 3.19F^{0.837}, \tag{4}$$

where Z_S = adjusted position of the surface inception point with origin at the critical section (corresponds to the extrapolation of [1] and [2], ideally located at the crest of the uncontrolled spillway), and $F = q/\sqrt{gs^3\sin\alpha}$. By adding the measured transition length (as defined in Fig. 3) to the length Z_S, dividing the result by s, and performing a new regression analysis led to Eq. 5 (which R=0.95). By performing then the ratio between the equation furnished by [2] and the present result, Eq. 6 was obtained.

$$\frac{z_L}{s} = 6.4F^{0.81}, \tag{5}$$

$$\frac{Z_B}{z_L} = 0.92F^{-0.01}, \tag{6}$$

where Z_B is the position calculated using the equation furnished by [2] and [3], $z_L=Z_S+L\sin\alpha$, and L=measured transition length. Equation 6 indicates a weak dependence on F, and suggests that the position of the peak of the biphasic wave observed in the present experiments is closely related to the position where the air concentration near the bottom is close to 1%. That is, the present methodology furnishes a simple way to obtain a measure of the inception point for the bed aeration. Details of the definition and quantification of the transition length may be found in [9], [18] and [20].

The length of the wave formed downstream of the superficial inception point was analyzed considering only the geometrical parameters of the flow, and then using Eqs. 1, 2 and 3 to relate it with F_r^*. The length of the wave is the distance between h_1 and h_3, and is set as L^o (see Fig. 8). Empirical relationships were tested using power laws, leading to Eqs. 7 and 8, which produced R = 0.95 and R = 0.89, respectively.

$$\frac{L^o}{k} = 6.12\left(\frac{L}{k}\right)^{0.636}, \tag{7}$$

$$\frac{L^o}{h_3} = 14.14\left(\frac{h_3}{h_2}\right)^{-4.94}. \tag{8}$$

L of Eq. 7 is the measured transition length shown in Fig. 3. The experimental ranges for the use of these equations are $8.49 \le L/k \le 42.43$ and $0.8 \le h_3/h_2 \le 0.95$, considering the 1V:1H ratio for the steps. From Eqs. 1, 2, and 3 it can be seen that L^o/k and L/k, can be obtained from the value of F_r^*.

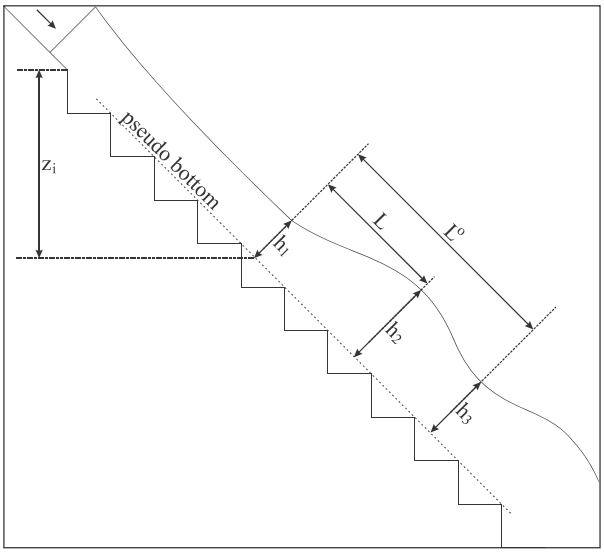

Fig. 8 Definitions of the pseudo bottom, depths (h_1, h_2 and h_3) and transition lengths (L and L^o)

C. Statistical Distributions, Uniform Flow and Extreme Values

The following Figs. 9 a and b are used in this analysis.

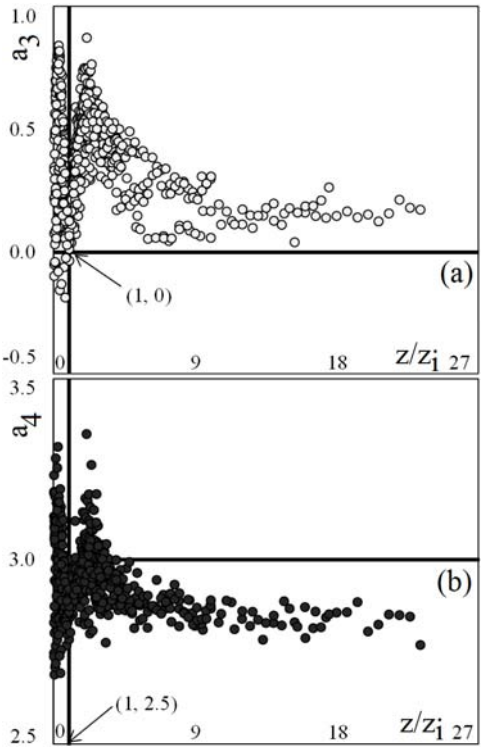

Fig. 9 Dimensionless central moments: (a) skewness, a_3 and (b) kurtosis, a_4

The use of acoustic sensors may also help to quantify the position of the so called "beginning of the uniform flow region" downstream from the superficial inception point. Uniform flow is, of course, approached, but never achieved. So, the "beginning of the uniform region" here considered is based on the apparent constancy of measured variables, and further compared with results of other authors. The present analysis considers the skewness and kurtosis factors of the measured data.

Figs. 9 a and b present the dimensionless third (skewness or a_3) and fourth (kurtosis or a_4) order central moments for the measured data without outliers. The dimensionless distance z/z_i is used in the figures, where z_i is the vertical position of the surface inception point, with origin at x=z=0 (see Fig. 1). Thus, $z/z_i<1$ indicates the single-phase flow region, for the S_2 profiles. Fig. 9a indicates that the distributions of values of h are predominantly right asymmetric (because the values are positive). Additionally, most of the points presented in Fig. 9b show predominance of platykurtic distributions.

Figs. 10a and 10b show the short growth and decay character of the asymmetry and kurtosis of the "h" data for $z/z_i<1$. Similarly, for $z/z_i>1$, Figs. 10c and 10d indicate that both parameters rise until a maximum (clearly visible for a_3), and that, after the peak, both a_3 and a_4 decay over distance.

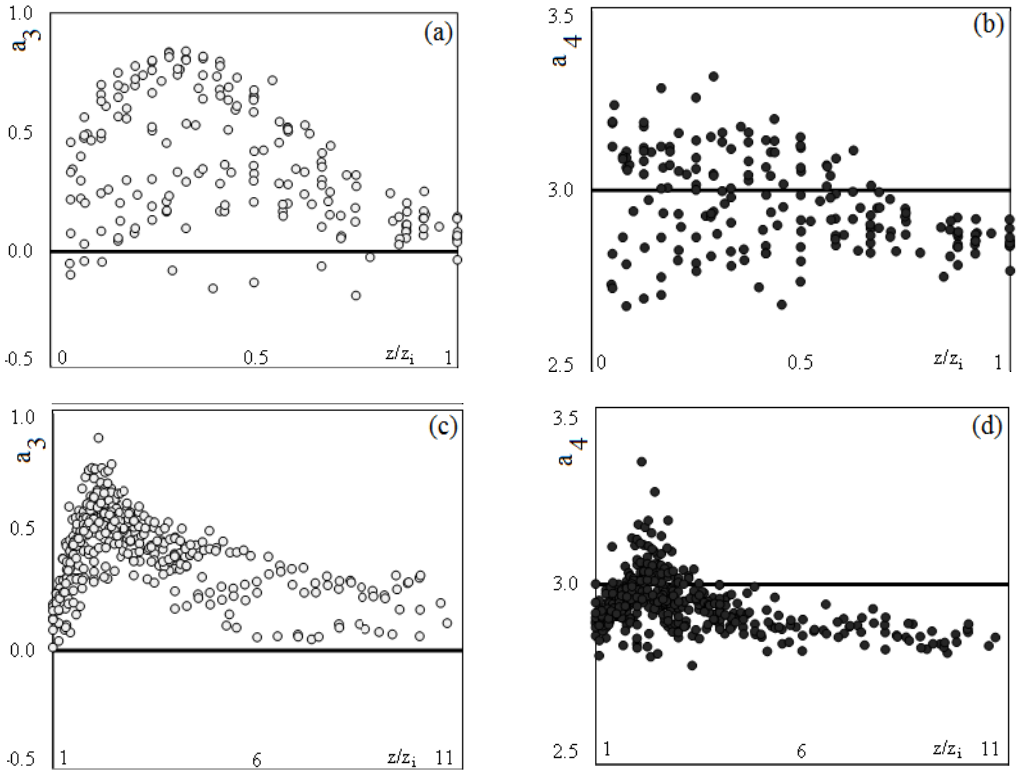

Fig. 10 Regions of variation of a_3 and a_4

The data presented in Figs. 9 and 10 suggest that the decay of a_3 and a_4 ends approximately at the position $z/z_i=z_u/z_i=10$. In order to compare the length of the decay region with literature results of the length needed to attain quasi-uniform flows, the origin x=z=0 was shifted to the position z_i, so that we can write $(z_u-z_i)/z_i=z_{ui}/z_i=9$, where $z_{ui}=z_u-z_i$. Equation 9 was obtained from a fit of the experimental data presented in Fig. 11, with R=0.91. Using $z_{ui}/z_i=9$ results in Eq. 10.

$$\frac{z_i}{s}=1.397F^{1.06}, \tag{9}$$

$$\frac{z_{ui}}{s}=12.6F^{1.06}. \tag{10}$$

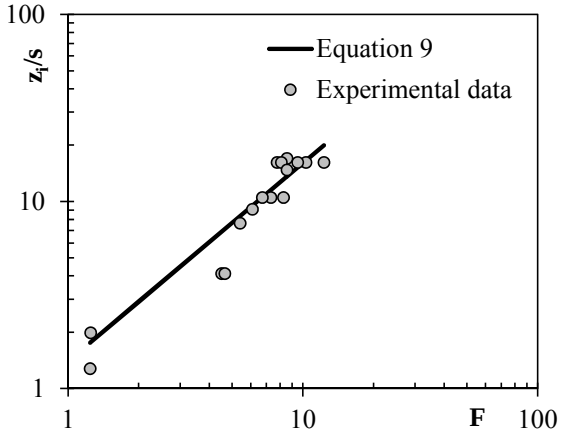

Fig. 11 Vertical position of the surface inception point, z_i

When considering Figs. 12 a, b, the decay of skewness and kurtosis statistics for the measurements appears to be concluded at approximately $z_{ui}/h_c\cong20$. This location will be proposed as the end of the decaying region of a_3 and a_4.

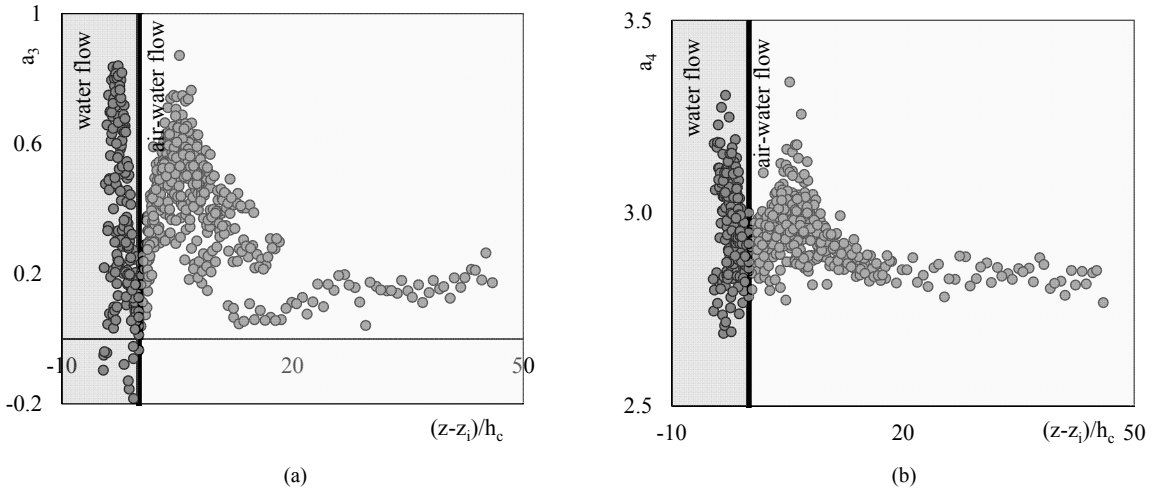

Fig. 12 Relationship between a_3, a_4 and $(z-z_i)/h_c$

Interestingly, [21] proposed that the uniform flow occurs for $z/h_c \geq 25$-30, using the slope 1V:0.75H. For the same slope, [22] indicated that the uniform flow occurs for $z/h_c \geq 20$. Employing the equation given by [3] for $\alpha=45°$, $z/h_c>19.04$. From experimental results, [7] concluded that the dimensionless vertical length required to occur quasi-uniform flow in stepped spillways depends on s/h_c and α. The equation given by [7] results in $z/h_c=24.95$ for $s/h_c=1$. There is general agreement in the literature to the skewness and kurtosis arguments establishing a "decay length" to aerated, uniform flow of $z_{ui}/h_c= 20$.

Further, adding the "decay length" of $z_{ui}/h_c \cong 20$ to Eq. 4 multiplied by s/h_c leads to Eq. 11:

$$\frac{z_{ui}}{h_c} + \overbrace{\frac{Z_S}{s}}^{Eq.4}\frac{s}{h_c} = 20 + \overbrace{3.19F^{0.837}}^{Eq.4}\frac{s}{h_c}. \quad (11)$$

Using $h_c=(q^2/g)^{1/3}$, Eq. 11 is simplified to

$$\frac{Z_u}{h_c} = 20 + 3.19\left(\frac{s}{h_c}\right)^{-0.26}(\sin\alpha)^{-0.42}. \quad (12)$$

Z_u represents the vertical distance from the crest of an uncontrolled stepped spillway until the position of the end of the decay of a_3 and a_4. Equation (12) presents the general characteristics mentioned by [7], i.e., the dependence of Z_u with s/h_c and α, and also reproduces the limiting value ~20. So, the data obtained with the ultrasound sensors are conducive to conclusions similar to those presented in the mentioned literature for the beginning of the uniform flow region.

Finally, the data obtained using the ultrasound sensors also allow an evaluation of the maximum mean depth along the chute, which is relevant for the design of the side walls. The maximum mean dimensionless depths of the time-averaged profiles, max(Γ), were related here to the dimensionless distances $(z-z_i)/h_c$, s/h_c, h_1/h_c, h_2/h_c, h_3/h_c, leading, respectively, to

a) Equation 13, which produced R=0.83 and valid for $3.35<(z-z_i)/h_c<24.62$.
b) Equation 14, valid for $0,21<s/h_c<0.97$ and R=0.85,
c) Equation 15, valid for $0.31<h_1/h_c<0.47$and R=0.84,
d) Equation 16, valid for $0.41<h_2/h_c<0.60$ and R=0.96,
e) Equation 17, valid for $0.36<h_3/h_c<0.49$ and R=0.92.

$$\max(\Gamma) = 0.0074(z - z_i)/h_c + 0.445, \quad (13)$$

$$\max(\Gamma) = 0.215(s/h_c) + 0.421, \quad (14)$$

$$\max(\Gamma) = 1.27(h_1/h_c) + 0.0454, \quad (15)$$

$$\max(\Gamma) = 1.09(h_2/h_c) - 0.0202, \quad (16)$$

$$\max(\Gamma) = 1.48(h_3/h_c) - 0.111. \quad (17)$$

Additionally, the maximum instantaneous values are important for the design of the side walls. These instantaneous values are denoted here by $\max(\Gamma^*)$, and are linearly related to $\max(\Gamma)$, accordingly to Eq. 18, with R=0.98 and valid for

$0.42<\max(\Gamma)<0.64$. For this range of $\max(\Gamma)$, the maximum instantaneous height varies between 0.565 h_c and 1.01 h_c, which indicates that the ejection of the droplets follows the magnitude of h_c. This finding is of practical importance, being a simple way to obtain practical equations for designers.

$$\max(\Gamma^*) = 2.0\max(\Gamma) - 0.275 . \tag{18}$$

D. Comparison between Observed and Predicted Two-phase Surface Profiles

Reference [19] presented a solution for the surface profiles of the single-phase region of the flow along chute channels, which was used together with Eq. 19, proposed by [2] for the depth averaged air concentration downstream of the bed inception point, to predict the position of the two-phase surface profiles. The complementary Eqs. 20 through 22, proposed by [23] and [3], were used in these semi-empirical calculations. The procedure was described by [14] and [24].

$$c_i = \{\tanh[5\times10^{-4}(100^o - \alpha)Z_i]\}^{1/3}, \tag{19}$$

$$C_i = 1.2\times10^{-3}(240^o - \alpha), \tag{20}$$

$$C_u = 0.75(\sin\alpha)^{0.75}, \tag{21}$$

$$Z_B / s = 5.90F^{0.8}, \tag{22}$$

where $c_i=[C(Z_i)-C_i]/(C_u-C_i)$; $C(Z_i)$ is the depth-averaged air concentration; C_i is the depth-averaged air concentration at inception point; C_u is the uniform depth-averaged air concentration, and $Z_i=(z-z_i)/h_c$.

Fig. 13 shows the comparison between the measured and the predicted profiles for the present experimental conditions, based on the literature information. It can be seen that, in general, the predictions do not reproduce the measured profiles. In some cases, most of the predicted profiles are located at higher positions than the measured profiles (for example, Figs. 13a and 13n). In other cases, the predicted profiles are located mainly at lower positions (for example, Figs. 13i, 13j, and 13k). Intermediate situations are also observed. Further, the calculations suggest a continuously growing of the two-phase water depth, while the observed behaviors do not consubstantiate this prediction.

Because the value of the depth of the two-phase region is relevant for engineering purposes (for example, when defining the height of the lateral walls in spillways), the lack of agreement in Fig. 13 indicates that measurements are important to furnish a real picture of the expected behavior of two-phase surfaces on stepped spillways.

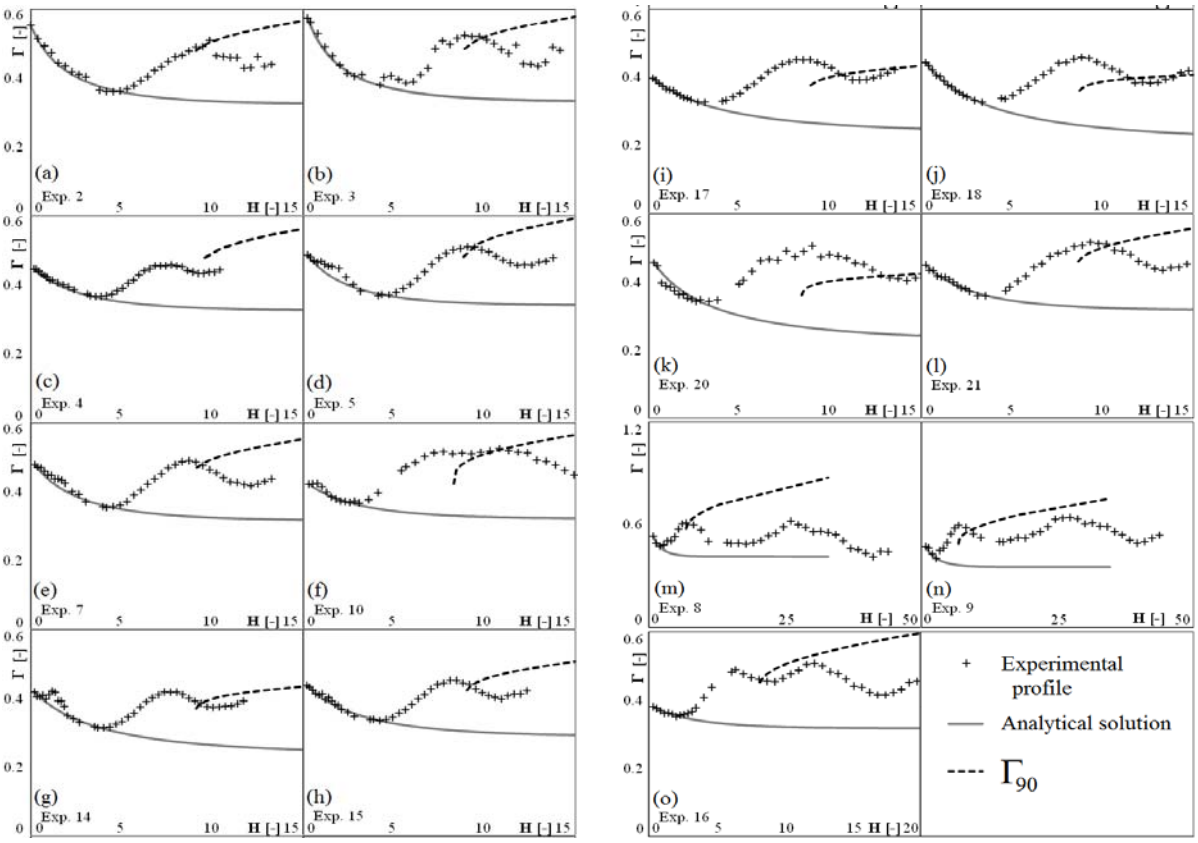

Fig. 13 Time-averaged free surface profiles and semi-empirical predictions for air-water depths (here $\Gamma=h_{90}/h_c$, h_{90}=flow depth at which C=90%, for C(y))

E. Turbulence Intensity and Strouhal Number

The fact that the flows under study occur along a stepped bed, that is, containing protuberances regularly shaped and separated, suggests that the statistical properties of the flow may be related to some characteristic frequencies along the channel. To verify this possibility, a Strouhal number was calculated for the flow, intending to verify possible correlations between the vertical turbulence intensity of the surface (as defined by [30]) and this nondimensional parameter (remembering that the Strouhal number is used to verify oscillating flow mechanisms). Note that the knowledge of the vertical displacements of the surface is important for design purposes. Further, it is observed that the turbulence of the white water region decays for greater distances to the inception point, so that the decay regions of the turbulence intensity and the Strouhal number are also quantified, and compared with the previous decay lengths. The time derivatives of the position of the free surface, denoted here by w, were used to evaluate the relative vertical turbulent intensity, w'/V_c, in which $w'=w_{rms}$ and $V_c=(gh_c)^{1/2}$ [30]. The fast Fourier transform was employed to obtain the dominant frequency, f_p, of the w values. This dominant frequency was then used to calculate the Strouhal number, defined as:

$$St = \frac{qf_p}{V^2} . \tag{23}$$

where q is the unit discharge, and $V = q/\bar{h}$ is the cross-sectional mean flow velocity. Reference [13] used the Strouhal number in the study of hydraulic jumps, which indicated the possibility of calculating it also in the present case of two-phase flows in chutes. It is emphasized that, in the present case, the aim was to verify if the vertical turbulence intensity of surface admits a correlation with the Strouhal number, and to evaluate the length of the decay region of both parameters.

Fig. 14 shows the main results of this analysis. Fig. 14a presents the relative intensities as a function of $(z-z_i)/h_c$. Four regions may be defined for the envelopes of the measured cloud of points, considering the sequence of increasing and decreasing behavior of the vertical turbulent intensity. Fig. 14b shows the data of Fig. 14a for $(z-z_i)/hc< 20$. The following regions are identified: (1) Single-phase growing region for $-4.5<(z-z_i)/h_c<-3.15$, (2) Single-phase decay region, for $-3.15<(z-z_i)/h_c<0$, (3) Two-phase growing region, limited by $0<(z-z_i)/h_c<5.3$, and (4) Two-phase decay region, for $5.3<(z-z_i)/h_c<20$. Note that the final decay position coincides with the aforementioned conclusions, i.e., $(z-z_i)/h_c=20$. Figs. 14c and 14d show the Strouhal number as a function of $(z-z_i)/h_c$. Although a greater spreading of the data is observed, in relation to the relative turbulent intensity, the envelopes of the cloud of points also follow the grow/decay pattern shown in Figs. 12a and b. As can be seen, the derivatives of the relative turbulence intensity and the Strouhal number change sign around the same position. The first change occurs at $(z-z_i)/h_c=0$, and the second change occurs around $(z-z_i)/h_c$~5-6. From these data, it is possible to suggest that both parameters are correlated, although no quantification of this correlation is presented here.

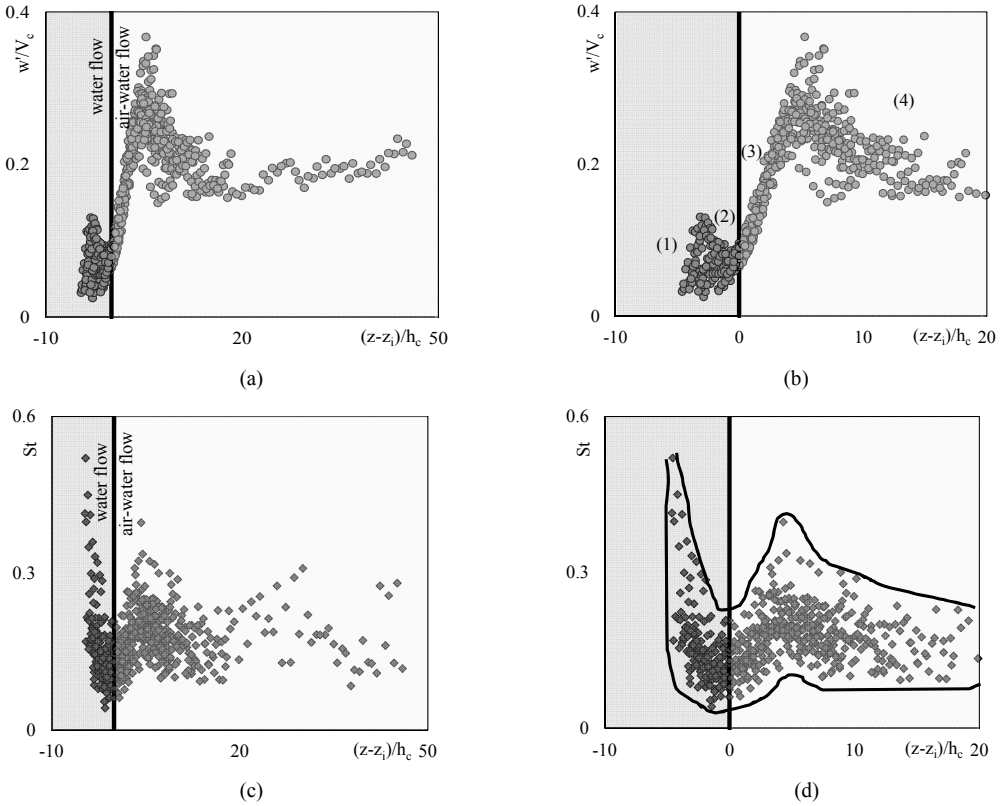

Fig. 14 Relative turbulent intensity (a,b) and Strouhal number (b,c). Fig. b shows the regions 1, 2, 3, and 4 discussed in the text, and Fig. d shows the similar trends for the upper and the lower envelope curves (adapted from [29])

Considering strong correlations between the two variables (Strouhal number and vertical intensity of the velocity), further equations for the dominant frequency will be needed in order to predict vertical turbulence intensities and vertical distances traveled by the surface (for design purposes). This analysis may also help to check numerical schemes devoted to the study of the breaking of the air-water interface and its evolution, as shown by [25].

IV. CONCLUSIONS

In this experimental study a methodology for the measurement of the position of the free surface was presented, using ultrasonic displacement meters. This method is suitable for obtaining water surface profiles of the average single-and two-phase flow, exposing, in the last case, a wavy shape. Considering the stationary wave, three characteristic depths were defined, the first of which coincides with the inception point of the superficial aeration. The present measurements confirm the results and equations proposed in the literature. The time-averaged profiles also enabled the development of characteristic correlations between the depths and length scales of the flow. The observed behavior of the coefficients of skewness and kurtosis enables a new methodology to define the "decay length", which is the length of spillway before uniform flow can be assumed. The method considers the decay of the mentioned statistical quantities. The same measurements also enabled the development of characteristic equations for the extreme values of the measured depths, which may be useful for the design of the confining walls of flows over stepped chutes. The comparison between observed and predicted two-phase surface profiles showed considerable deviations between both profiles, indicating that measurements are still important for the understanding of such flows. Finally, the Strouhal number and the vertical turbulent intensity, obtained from the fluctuations of the position of the free surface, showed similar behavior (that is, both parameters are correlated) and that the end of the decay in the graphs of the Strouhal number and the vertical relative intensity also agree with the point in the chute where uniform flow can be assumed.

ACKNOWLEDGMENT

The authors thank the Brazilian institutions CNPq (141078/2009-0), CAPES (AEX 0679/11-9) and FAPESP (10/52071-0) for financial support of this research, and also to Mr. Alcino de Paula, for important help during the measurements.

REFERENCES

[1] R.M. Boes, "Two-phase flow and energy dissipation on cascades" [Zweiphasenströmung und Energie umsetzung an Grosskaskaden], Doctoral Dissertation (Dr. sc. techn.), ETH Zurich, Switzerland, 2000.

[2] R.M. Boes, and W.H. Hager, "Two-phase flow characteristics of stepped spillways", J. Hydraul. Eng., vol. 129(9), pp. 661–570, 2003a.

[3] R.M. Boes, and W.H. Hager, "Hydraulic design of stepped spillways", ASCE, J. Hydraul. Eng., vol. 129(9), pp.671-679, 2003b.

[4] H. Chanson, The hydraulics of stepped chutes and spillways. A.A. Balkema, 2002.

[5] M.L Lueker, O. Mohseni, J.S. Gulliver, H.E. Schulz, and R.A. Christopher, "The physical model study of the Folsom Dam auxiliary spillway system", St. Anthony Falls Lab. Project Report 511.University of Minnesota, Minneapolis, MN, 2008.

[6] J. Matos, "Hydraulic design of stepped spillways over RCC dams", Proc., Int. Workshop on Hydraulics of Stepped Spillways, VAW, ETH Zurich, H.-E. Minor and W.H. Hager, eds., Balkema, Rotterdam, The Netherlands, pp. 187-194, 2000.

[7] I. Ohtsu, Y. Yasuda, M. Takahashi, "Flows characteristics of skimming flows in stepped channels", ASCE, J. Hydraul. Eng., 1 vol. 30(9), pp. 860-869, 2004.

[8] M. Pfister, and W.H. Hager, "Self-entrainment of air on stepped spillways", International Journal of Multiphase Flow, vol. 37(2), pp. 99-107, 2010.

[9] A.L.A. Simões, H.E. Schulz, and R.M. Porto, "Transition length between water and air-water flows on stepped chutes", Proc. 6th International Conference on Computational and Experimental Methods in Multiphase and Complex Flow, WITpress, UK, pp. 95-105, 2011a.

[10] P.H. Povh, "Evaluation of residual energy downstream of stepped spillways in skimming flows" [Avaliação da energia residual a jusante de vertedouros em degraus com fluxos em regime skimming flow], MSc Thesis, Department of Technology, Federal University of Paraná, Curitiba, Brazil [in Portuguese], 2000.

[11] D.G. Sanagiotto, "Flow characteristics in stepped spillways of slope 1V:0.75H" [Características do escoamento sobre vertedouros em degraus de declividade 1V:0.75H], MSc. Thesis. Institute of Hydraulic Research, Federal University of Rio Grande do Sul, Porto Alegre, Brazil, [in Portuguese], 2003.

[12] M.J. Tozzi, "Characterization of flow behavior in stepped spillways" [Caracterização/comportamento de escoamentos em vertedouros com paramento em degraus], Dr. Thesis. University of São Paulo, Brazil, [in Portuguese], 1992.

[13] F. Murzyn, and H. Chanson, "Free-surface fluctuations in hydraulic jumps: Experimental observations", Experimental Thermal and Fluid Science, vol. 33, pp. 1055-1064, 2009.

[14] A.L.A. Simões, H.E. Schulz, and R.M. Porto, Reply on "Stepped and smooth spillways: resistance effects on stilling basin lengths", Journal of Hydraulic Research, vol. 49(3), pp. 407–408 (DOI: 10.1080/00221686.2011.568199), 2011b.

[15] V.T. Chow, Open channel hydraulics. McGraw-Hill, New York, USA, 1959.

[16] S.C. Wilhelms, and J.S.; Gulliver (2005) "Bubbles and waves description of self-aerated spillway flow", Journal of Hydraulic Research, vol. 43(5), pp. 522-531, 2005.

[17] E. Kreyszig, Advanced engineering mathematics, LTC, 9th ed. vol. 3, Rio de Janeiro, Brazil [Portuguese edition], 2009.

[18] H.E. Schulz, and A.L.A. Simões, "Alternative fomulation for transition lengths: analogies with basic equation of Transport Phenomena" [Equacionamento alternativo para comprimentos de transição: analogias com equações básicas de Fenômenos de Transporte] Technical Report, School of Engineering at São Carlos, University of São Paulo, available online: vertedoresemdegraus.blogspot.com;stoa.usp.br/ltr/files/ and in http://stoa.usp.br/hidraulica/files/-1/16207/Schulz_H.E._Simões_A.L.A_LTR-Relatório+I_II_11.pdf [in Portuguese], 2011.

[19] A.L.A. Simões, H.E. Schulz, and R.M. Porto, "Stepped and smooth spillways: resistance effects on stilling basin lengths" Journal of Hydraulic Research, vol. 48(3), pp. 329-337, 2010.

[20] A.L.A Simões, "Stepped chutes: Theoretical experimental and numerical study" [Canais e vertedores em degraus: Estudo teórico, experimental e numérico], Dr. Thecnical Report, 157 p. University of São Paulo, Brazil, [in Portuguese], 2011.

[21] J. Matos, and A. Quintela, "Guidelines for the hydraulic design of stepped spillways for concrete dams", ICOLD Energy Dissipation Bull, 1995.

[22] D. Yildiz, and I. Kas, "Hydraulic performance of stepped chute spillways", Hydropower Dams, vol. 5(4), pp. 64–70, 1998.

[23] W.H. Hager, "Uniform aerated chute flow", J. Hydraul. Eng., vol. 117(4), pp. 528–533, 1991.

[24] M. Takahashi, and I. Ohtsu, Discussion on "Stepped and smooth spillways: resistance effects on stilling basin lengths", Journal of Hydraulic Research, vol. 49(3), pp. 404-408. (DOI: 10.1080/00221686.2011.568200), 2011.

[25] H.E. Schulz, R.J. Lobosco, and A.L.A. Simões, "Multiphase analysis of entrained air in skimming flows along stepped chutes" Fifth International Conference on Advanced COmputational Methods in ENgineering (ACOMEN 2011), Liège, Belgium, 14-17 November. University of Liège, 2011. Available online:

[26] http://www.ltas.ulg.ac.be/acomen2011/NewWebSite/docs/Abstracts/Fluvial_hydraulics/Fluvial%20hydraulics10.pdf

[27] E.J. Arantes, Characterizing flows along stepped spillways through CFD [Caracterização do escoamento sobre vertedores em degraus via CFD], Dr. Thesis. School ef engineering at São Carlos, University of São Paulo, Brazil, [in Portuguese], 204 p., 2007.

[28] E.J. Arantes, R.M. Porto, J.S. Gulliver, A.C.M. Lima, and H.E. Schulz, "Lower nape aeration in smooth channels: experimental data and numerical simulation", Annals of the Brazilian Academy of Sciences (Anais da Academia Brasileira de Ciências), vol. 82(2), pp. 521-537, 2010.

[29] J. Matos, "Emulsification of the air and energy dissipation of flows in stepped spillways" [Emulsionamento de ar e dissipação de energia do escoamento em descarregadores em degraus], Dr. Thesis, Instituto Superior Técnico, Portugal, 1999.

[30] A.L.A Simões, "Turbulent Flows in stepped chutes: Experimental data, numerical solutions and theoretical propositions" [Escoamentos turbulentos em canais com o fundo em degraus: Resultados experimentais, soluções numéricas e proposições teóricas], Dr. Thesis, School of Engineering at São Carlos, University of São Paulo, Brazil, [in Portuguese], 2012.

[31] A.L.A Simões, H.E. Schulz, R.J. Lobosco, and R.M. Porto, "Stepped spillways: Theoretical, experimental and numerical studies", H.E. Schulz, A.L.A. Simões, R.J. Lobosco, Eds., Hydrodynamics: Natural Water Bodies, Intech open, Rijeka, Croatia, pp. 237-262, 2011.